MOLECULAR AGGREGATION CHARACTERIZED BY HIGH ORDER AUTOCORRELATION IN FLUORESCENCE CORRELATION SPECTROSCOPY

ARTHUR G. PALMER III AND NANCY L. THOMPSON
Department of Chemistry, University of North Carolina at Chapel Hill, Chapel Hill, North Carolina 27514

ABSTRACT The use of high order autocorrelation in fluorescence correlation spectroscopy for investigating aggregation in a sample that contains fluorescent molecules is described. Theoretical expressions for the fluorescence fluctuation autocorrelation functions defined by $G_{m,n}(\tau) = [\langle \delta F^m(t+\tau)\delta F^n(t)\rangle - \langle \delta F^m(t)\rangle \langle \delta F^n(t)\rangle]/\langle F\rangle^{m+n}$, where $\delta F(t)$ is the fluorescence fluctuation at time t, $\langle F\rangle$ is the average fluorescence, and m and n are integers less than or equal to 3, are derived. Methods for determining the number densities and relative fluorescence yields of aggregates of different sizes from a series of $G_{m,n}(0)$ values are outlined. The method is applied to 1,1′-dioctadecyl-3,3,3′,3′-tetramethylindocarbocyanine perchlorate suspended in solutions of water and ethyl alcohol. The technique presented may prove useful in detecting and characterizing aggregates of fluorescent-labeled biological molecules such as cell surface receptors.

INTRODUCTION

Aggregation of biological macromolecules occurs in a number of processes such as the interaction of hormones (Cuatrecasas, 1983; Pastan and Willingham, 1981), neurotransmitters (Axelrod et al., 1976*a*), growth factors (Schlessinger et al., 1978) and antibodies (Metzger, 1978) with cell surface receptors, and assembly of the cytoplasmic matrix (Frieden, 1985). Electron microscopy (Uzgiris and Kornberg, 1983; Roos et al., 1983; Shotton et al., 1978), fluorescence energy transfer (Uster and Pagano, 1986; Watts et al., 1986; Schreiber et al., 1980), fluorescence photobleaching recovery (Lanni et al., 1981; Salmon et al., 1984), digital video optical microscopy (Gross and Webb, 1986), and co-precipitation by monoclonal antibodies (Due et al., 1986) have provided information about molecular association in biological systems; however, new experimental techniques may provide additional insights into the mechanism and function of association.

In fluorescence correlation spectroscopy (FCS; Magde et al., 1974; Elson and Magde, 1974) the temporal autocorrelation of fluctuations in fluorescence emitted from a small illuminated volume in a sample containing mobile fluorescent molecules provides information about rates of transport through the illuminated volume and rates of chemical reactions occurring in the sample. FCS has been applied to the kinetics of binding of the dye ethidium bromide to DNA (Magde et al., 1972; Magde et al., 1974; Sorscher et al., 1980; Icenogle and Elson, 1983*a*,*b*), to the motion of myosin fragments during actin-activated ATPase (Borejdo, 1979), to the assumption of different orientations by myosin subfragment 1 in contracting muscle fibers (Borejdo et al., 1979), to immunoglobulin surface-binding kinetics (Thompson and Axelrod, 1983), to fluorescence immunoassays (Briggs et al., 1981; Nicoli et al., 1980), to the detection and classification of viruses (Hirschfeld and Block, 1977; Hirschfeld et al., 1977), to measurement of lateral diffusion coefficients of fluorescent dyes in model biological membranes (Fahey et al., 1977; Fahey and Webb, 1978), and to measurement of the sizes of focused laser beams (Sorscher and Klein, 1980).

In a recent application of FCS, called Scanning-FCS (Petersen, 1984, 1986; Petersen, et al., 1986), a sample containing immobile aggregates of fluorescent molecules is translated through the illuminated volume. Under certain conditions, the extrapolated time-zero value of the autocorrelation of fluorescence fluctuations, given by

$$g(\tau) = \frac{\langle F(t+\tau)F(t)\rangle - \langle F(t)\rangle^2}{\langle F(t)\rangle^2} = \frac{\langle \delta F(t+\tau)\delta F(t)\rangle}{\langle F(t)\rangle^2}, \quad (1)$$

where $F(t)$ is the fluorescence at time t, $\langle F(t)\rangle$ is the average fluorescence, and $\delta F(t) = F(t) - \langle F(t)\rangle$ is the fluctuation of the fluorescence at time t from its average value, provides an estimate of the mean number of aggregates per area and the mean number of monomers per aggregate. Scanning-FCS has been used to examine virus glycoprotein aggregation on cell surfaces (Petersen et al., 1986).

As shown in this paper, the time-zero values of a series of high order fluorescence fluctuation autocorrelation func-

tions $G_{m,n}(\tau)$, defined as[1]

$$G_{m,n}(\tau) = \frac{\langle \delta F^m(t+\tau)\delta F^n(t)\rangle - \langle \delta F^m(t)\rangle \langle \delta F^n(t)\rangle}{\langle F(t)\rangle^{m+n}}, \quad (2)$$

can provide additional information about the average number densities and relative fluorescence yields of the fluorescent species in the observed volume.[2] After the following theoretical discussion of high order fluorescence fluctuation autocorrelation functions in FCS, the use of these functions to investigate the aggregation of the fluorescent lipid 1,1′-dioctadecyl-3,3,3′,3′-tetramethylindocarbocyanine perchlorate (diI) suspended in different mixtures of water and ethyl alcohol is described.

High order autocorrelation functions similar to those defined in Eq. 2 have found use in photoelectron statistics (Saleh, 1978), light scattering (Pusey, 1977; Oliver, 1981), analysis of electrical noise associated with membrane channels (Leibovitch and Fischbarg, 1985, 1986; Leibovitch et al., 1985), and statistical mechanics of condensed phases (Ackerson et al., 1985). High order autocorrelation functions with m unequal to n have also been proposed as a technique for investigating the time-reversal properties of a fluctuating system (Pomeau, 1982; Steinberg, 1986). The proceedings of a workshop on high order correlation functions have recently been published (Suck et al., 1985).

THEORETICAL BASIS

In the following sections, expressions for the functions $G_{m,n}(\tau)$ defined in Eq. 2 are derived. The dependence of the values of $G_{m,n}(0)$ on the distribution of particles with different measured values of fluorescence is examined, and methods of determining this distribution from experimentally obtained quantities $G_{m,n}(0)$ are outlined.

General Expression for High Order Fluorescence Fluctuation Autocorrelation Functions

In the experimental arrangement considered, a small area of a two-dimensional sample that contains a number of fluorescent chemical species with different effective fluorescence yields is illuminated. Molecules of the ith species are transported through the illuminated (and observed) area by diffusion in the x, y-plane with coefficient D_i and uniform translation along the y-axis with speed V. The solution is assumed to be ideal and to be in equilibrium. Chemical reactions between species, e.g., aggregation kinetics, are not treated.

The fluorescence $F(t)$, the average fluorescence $\langle F\rangle$, and the fluorescence fluctuation $\delta F(t)$ are given by

$$F(t) \propto \sum_{i-1}^{R} Q_i \int I(\mathbf{r})\, C_i(\mathbf{r}, t)\, \mathrm{d}^2 r \quad (3a)$$

$$\langle F\rangle \propto \sum_{i-1}^{R} Q_i \langle C_i\rangle \int I(\mathbf{r})\, \mathrm{d}^2 r \quad (3b)$$

$$\delta F(t) \propto \sum_{i-1}^{R} Q_i \int I(\mathbf{r})\, \delta C_i(\mathbf{r}, t)\, \mathrm{d}^2 r, \quad (3c)$$

where the "fluorescence yields" Q_i are the products of the absorptivities, quantum efficiencies, and experimental fluorescence collection efficiencies of molecules of the ith species, $I(\mathbf{r})$ is proportional to the intensity profile of the exciting light and the transmission function of observation, $C_i(\mathbf{r}, t)$ is the concentration of the ith chemical species at position $\mathbf{r}$ and time t, R is the number of fluorescent species, and integration over all two-dimensional space is denoted by $\int \mathrm{d}^2 r$. Also in Eqs. 3,

$$\delta C_i(\mathbf{r}, t) = C_i(\mathbf{r}, t) - \langle C_i\rangle \quad (4)$$

is the spatial and temporal fluctuation of the concentration $C_i(\mathbf{r},t)$ from its average value $\langle C_i\rangle$.

Using Eqs. 3b and 3c in Eq. 2, and noting that the average properties of a stationary signal are independent of the origin of time,

$$\begin{aligned} G_{m,n}(t) = &\left(\sum_{i-1}^{R} Q_i \langle C_i\rangle \int I(\mathbf{r})\, \mathrm{d}^2 r\right)^{-(m+n)} \\ &\cdot \sum_{i_1-1}^{R}\sum_{i_2-1}^{R} \cdots \sum_{i_{m+n}-1}^{R} Q_{i_1} Q_{i_2} \cdots Q_{i_{m+n}} \\ &\cdot \int\int \cdots \int I(\mathbf{r}_1) I(\mathbf{r}_2) \cdots I(\mathbf{r}_{m+n}) \\ &\cdot g_{m,n}(i_1, i_2, \ldots, i_{m+n}; \mathbf{r}_1, \mathbf{r}_2, \ldots, \mathbf{r}_{m+n}; t) \\ &\cdot \mathrm{d}^2 r_1 \mathrm{d}^2 r_2 \cdots \mathrm{d}^2 r_{m+n}, \end{aligned} \quad (5)$$

where

$$\begin{aligned} &g_{m,n}(i_1, i_2, \ldots, i_{m+n}; \mathbf{r}_1, \mathbf{r}_2, \ldots, \mathbf{r}_{m+n}; t) \\ &= \langle \delta C_{i_1}(\mathbf{r}_1, t)\delta C_{i_2}(\mathbf{r}_2, t)\cdots\delta C_{i_m}(\mathbf{r}_m, t) \\ &\quad \cdot \delta C_{i_{m+1}}(\mathbf{r}_{m+1}, 0)\delta C_{i_{m+2}}(\mathbf{r}_{m+2}, 0)\cdots\delta C_{i_{m+n}}(\mathbf{r}_{m+n}, 0)\rangle \\ &\quad - \langle \delta C_{i_1}(\mathbf{r}_1, t)\delta C_{i_2}(\mathbf{r}_2, t)\cdots\delta C_{i_m}(\mathbf{r}_m, t)\rangle \\ &\quad \cdot \langle \delta C_{i_{m+1}}(\mathbf{r}_{m+1}, 0)\delta C_{i_{m+2}}(\mathbf{r}_{m+2}, 0)\cdots\delta C_{i_{m+n}}(\mathbf{r}_{m+n}, 0)\rangle. \end{aligned} \quad (6)$$

For systems in equilibrium, the autocorrelation functions are even in time (Steinberg, 1986); therefore $G_{n,m}(t)$ equals $G_{m,n}(t)$ and only autocorrelation functions for which $m \leq n$ are considered. As shown in Appendix A, the functions $g_{m,n}$

[1] In generalizing Eq. 1, a number of possible offset values (i.e., the second term of the numerator in Eq. 2) and normalizations (i.e., the denominator in Eq. 2) might be chosen. The mth, nth-order autocorrelation function of fluorescence fluctuations $G_{m,n}(\tau)$ has been defined according to Eq. 2 because the choice of offset value ensures that $G_{m,n}(\tau)$ tends towards zero as τ approaches infinity. The choice of normalization in Eq. 2 allows simpler algebraic expressions in the denominators of the $G_{m,n}(0)$ that are later calculated (Eq. 18).

[2] If the fluctuations about the average value of a stationary signal have a Gaussian distribution, then high order autocorrelation functions of fluctuations in the signal, such as those defined in Eq. 2, are determined by $G_{1,1}(\tau)$, and the high order autocorrelation functions provide no new information (Saleh, 1978; Oliver, 1981). The distribution of fluctuations in fluorescence emitted from a small illuminated volume depends in a complex manner on the fluorescence yields and number densities of the fluorescent species in the sample. A sufficient condition for the distribution to be non-Gaussian is that the number densities of all of the fluorescent species be small enough that number fluctuations in the illuminated volume are characterized by Poisson statistics.

can be written as sums of products of Kronecker deltas of species indices and the single species correlation functions

$$f_{m,n}(i, \mathbf{r}_1, \mathbf{r}_2, \ldots \mathbf{r}_{m+n}; t) = g_{m,n}(i, i, \ldots, i; \mathbf{r}_1, \mathbf{r}_2, \ldots, \mathbf{r}_{m+n}; t). \quad (7)$$

Defining $F_{m,n}(i, t)$ as the autocorrelation function $G_{m,n}(t)$ when only the ith species is present,

$$F_{m,n}(i, t) = (\langle C_i \rangle \int I(\mathbf{r})\, \mathrm{d}^2 r)^{-(m+n)} \cdot \int\int \cdots \int I(\mathbf{r}_1) I(\mathbf{r}_2) \cdots I(\mathbf{r}_{m+n}) \cdot f_{m,n}(i; \mathbf{r}_1, \mathbf{r}_2, \ldots, \mathbf{r}_{m+n}; t)\, \mathrm{d}^2 r_1\, \mathrm{d}^2 r_2 \cdots \mathrm{d}^2 r_{m+n}, \quad (8)$$

and using Eqs. A3 in Eq. 5, results in the following expressions for the multiple species high order fluorescence fluctuation autocorrelation functions $G_{m,n}(t)$ in terms of the single species high order fluorescence fluctuation autocorrelation functions $F_{m,n}(i, t)$:

$$K^{(m+n)} G_{m,n}(t) = \sum_{i=1}^{R} X_{m,n}(i, t), \quad \text{for } (m, n) = (1, 1) \text{ and } (1, 2);$$

$$K^4 G_{2,2}(t) = \sum_{i=1}^{R} [X_{2,2}(i, t) - 2X_{1,1}^2(i, t)] + 2\left[\sum_{i=1}^{R} X_{1,1}(i, t)\right]^2;$$

$$K^4 G_{1,3}(t) = \sum_{i=1}^{R} [X_{1,3}(i, t) - 3X_{1,1}(i, t) X_{1,1}(i, 0)] + 3 \sum_{i=1}^{R} \sum_{j=1}^{R} X_{1,1}(\mathrm{i}, t) X_{1,1}(j, 0);$$

$$K^5 G_{2,3}(t) = \sum_{i=1}^{R} [X_{2,3}(i, t) - 6X_{1,1}(i, t) X_{1,2}(i, t) - 3X_{1,1}(i, 0) X_{1,2}(i, t)] + \sum_{i=1}^{R} \sum_{j=1}^{R} [6X_{1,1}(i, t) X_{1,2}(j, t) + 3X_{1,1}(i, 0) X_{2,1}(j, t)];$$

$$K^6 G_{3,3}(t) = \sum_{i=1}^{R} [X_{3,3}(i, t) - 6X_{1,1}(i, 0) X_{1,3}(i, t) - 9X_{1,1}(i, t) X_{2,2}(i, t) - 9X_{1,2}^2(i, t) + 9X_{1,1}(i, t) X_{1,1}^2(i, 0) + 12X_{1,1}^3(i, t)] + \sum_{i=1}^{R} \sum_{j=1}^{R} [6X_{1,1}(i, 0) X_{1,3}(j, t) + 9X_{1,1}(i, t) X_{2,2}(j, t) + 9X_{1,2}(i, t) X_{1,2}(j, t) - 18X_{1,1}^2(i, t) X_{1,1}(j, t) - 18X_{1,1}(i, 0) X_{1,1}(i, t) X_{1,1}(j, 0)] + \sum_{i=1}^{R} \sum_{j=1}^{R} \sum_{k=1}^{R} X_{1,1}(i, t) \cdot [9X_{1,1}(j, 0) X_{1,1}(k, 0) + 6X_{1,1}(j, t) X_{1,1}(k, t)]; \quad (9)$$

where

$$K = \sum_{i=1}^{R} Q_i \langle N_i \rangle, \quad (10)$$

$$X_{m,n}(i, t) = Q_i^{m+n} \langle N_i \rangle^{m+n} F_{m,n}(i, t), \quad (11)$$

$$\langle N_i \rangle = 2 \langle C_i \rangle \int [I(\mathbf{r})/I_0]\, \mathrm{d}^2 r, \quad (12)$$

I_0 is the maximum intensity, and $\langle N_i \rangle$ is the average number of particles of the ith species in the observation area, defined to be consistent with Elson and Magde (1974).

The $F_{m,n}(i, t)$ are determined from Eq. 8 and the $f_{m,n}(\mathrm{i}; \mathbf{r}_1, \mathbf{r}_2, \ldots \mathbf{r}_{m+n}; t)$, which are derived in Appendix B. Using Eqs. B11 in Eq. 8, and assuming a Gaussian shape for the spatial illumination profile, i.e.,

$$I(\mathbf{r}) = I_0 \exp(-2\, r^2/s^2), \quad (13)$$

where s is a constant, gives the following results for the single species fluorescence fluctuation autocorrelation functions:

$$\begin{aligned} F_{m,n}(i, t) &= L_{m,n}(i, t) \text{ for } (m, n) = (1, 1) \text{ and } (1, 2) \\ F_{2,2}(i, t) &= L_{2,2}(i, t) + 2L_{1,1}^2(i, t) \\ F_{1,3}(i, t) &= L_{1,3}(i, t) + 3L_{1,1}(i, t)/\langle N_i \rangle \\ F_{2,3}(i, t) &= L_{2,3}(i, t) + 3L_{1,2}(i, t)/\langle N_i \rangle + 6L_{1,1}(i, t) L_{1,2}(i, t) \\ F_{3,3}(i, t) &= L_{3,3}(i, t) + 6L_{1,3}(i, t)/\langle N_i \rangle + 9L_{1,1}(i, t) L_{2,2}(i, t) \\ &\quad + 9L_{1,2}^2(i, t) + 9L_{1,1}(i, t)/\langle N_i \rangle^2 + 6L_{1,1}^3(i, t), \end{aligned} \quad (14)$$

where

$$L_{m,n}(i, t) = \frac{2^{m+n-1} \exp[-2mn(t/\tau_f)^2/(m+n+2mnt/\tau_{D_i})]}{\langle N_i \rangle^{m+n-1} (m+n+2mnt/\tau_{D_i})} \quad (15)$$

and

$$\tau_{D_i} = s^2/4D_i$$
$$\tau_f = s/V. \quad (16)$$

The complete expressions for $G_{m,n}(t)$ can be obtained by substituting Eqs. 11, 14, and 15 into Eqs. 9.

Time-Zero Values of High Order Fluorescence Fluctuation Autocorrelation Functions

Evaluating Eqs. 9, 11, 14, and 15 at time zero gives

$$\begin{aligned} G_{1,1}(0) &= B_2 \\ G_{1,2}(0) &= 4B_3/3 \\ G_{2,2}(0) &= 2B_4 + 2B_2^2 \\ G_{1,3}(0) &= 2B_4 + 3B_2^2 \\ G_{2,3}(0) &= 16B_5/5 + 12B_2B_3 \\ G_{3,3}(0) &= 16B_6/3 + 30B_2B_4 + 15B_2^3 + 16B_3^2, \end{aligned} \quad (17)$$

where

$$B_k = \frac{\sum_{i=1}^{R} \alpha_i^k \langle N_i \rangle}{\left[\sum_{i=1}^{R} \alpha_i \langle N_i \rangle\right]^k} \tag{18}$$

are constants, and

$$\alpha_i = Q_i/Q_1 \tag{19}$$

is the relative fluorescence yield of the ith species.

Fig. 1 *a* shows the theoretical values of $G_{m,n}(0)$ calculated from Eqs. 17 and 18 for one species. As shown, for $\langle N_1 \rangle \gg 1$, $G_{1,1}(0)$ decreases as $\langle N_1 \rangle^{-1}$; $G_{1,2}(0)$, $G_{2,2}(0)$, and $G_{1,3}(0)$ decrease as $\langle N_1 \rangle^{-2}$; and $G_{2,3}(0)$ and $G_{3,3}(0)$ decrease as $\langle N_1 \rangle^{-3}$. Assuming an experimental detection limit of $G_{m,n}(0) > 0.0001$ (Thompson and Axelrod, 1983), $G_{1,1}(0)$ can be measured for $\langle N_1 \rangle < 10^4$, the second set of $G_{m,n}(0)$ values can be measured for $\langle N_1 \rangle < 100$, and the third set of $G_{m,n}(0)$ values can be measured for $\langle N_1 \rangle < 50$.

If the average total number of molecules $\langle N \rangle$ in the observed area is known, and if oligomers of p molecules have relative fluorescence yields of $\alpha_p = p$, then, referring to Eqs. 17 and 18, $G_{1,1}(0) \geq \langle N \rangle^{-1}$. If the inequality is found to hold, some aggregation has occurred. Alternatively, if the average total number of molecules in the observed area is not known, then a set of measured values $G_{m,n}(0)$ that is not consistent with a set of numbers shown in Fig. 1 *a*, for some value of $\langle N_1 \rangle$, implies a heterogeneous sample.

The time-zero values of autocorrelation functions can be sensitive to changes in molecular aggregation. Computer simulations (Petersen, 1986) have indicated that $G_{1,1}(0)$ can be significantly affected by a change in mean aggregate size from one to five to ten monomers. As an additional example, consider the value of $G_{1,1}(0)$ when a total of 1,000 molecules are present in two species and when the relative effective fluorescence yields of oligomers of p molecules are $\alpha_p = p$ (e.g., when the molecules are present as monomers and as hexamers with $\alpha_2 = 6$), such that $1{,}000 = \langle N_1 \rangle + \alpha_2 \langle N_2 \rangle$. Fig. 1 *b* shows the theoretical values of $G_{1,1}(0)$ calculated from Eqs. 17 and 18 as a function of $\langle N_2 \rangle$ and α_2. If all molecules are present as monomers, $G_{1,1}(0) = 0.001$. Assuming a 5–10% accuracy in the determination of $G_{1,1}(0)$, then (as shown) a single aggregate of 10 molecules ($\alpha_2 = 10$, $\langle N_2 \rangle = 1$), 10 aggregates of trimers ($\alpha_2 = 3$, $\langle N_2 \rangle = 10$), or 25 aggregates of dimers ($\alpha_2 = 2$, $\langle N_2 \rangle = 25$) can theoretically be detected in the $G_{1,1}(0)$ value. More extensive aggregation results in increases by factors as large as 100 in the measured valued of $G_{1,1}(0)$.

Although calculating the time dependence of the $G_{m,n}(t)$ for illumination profiles $I(\mathbf{r})$ not given by Eq. 13 is rather complex (Axelrod et al., 1976*b*), expressions for the $G_{m,n}(0)$ for other illumination profiles $I(\mathbf{r})$ can be readily obtained. Using Eqs. B11, evaluated at time zero according to Eq. B10, in Eqs. 8, 9, and 11, results in the following expressions for $G_{m,n}(0)$:

$$G_{1,1}(0) = 2h_2B_2$$

$$G_{1,2}(0) = 4h_3B_3$$

$$G_{2,2}(0) = 8h_4B_4 + 8h_2^2B_2^2$$

$$G_{1,3}(0) = 8h_4B_4 + 12h_2^2B_2^2$$

$$G_{2,3}(0) = 16h_5B_5 + 72h_2h_3B_2B_3$$

$$G_{3,3}(0) = 32h_6B_6 + 240h_2h_4B_2B_4 + 120h_2^3B_2^3 + 144h_3^2B_3^2, \tag{20}$$

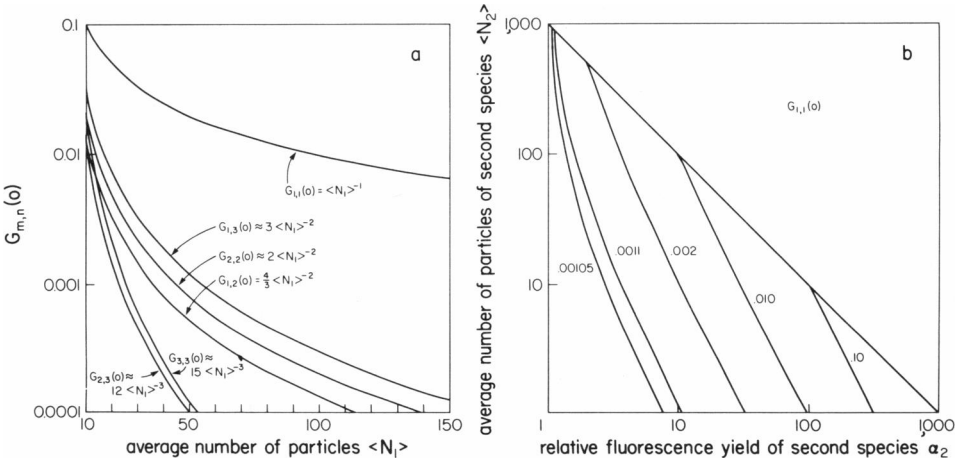

FIGURE 1 Theoretical time-zero values of high order fluorescence fluctuation autocorrelation functions. (*a*) Shown are the values of $G_{m,n}(0)$ for a monodisperse sample, as a function of the average number of particles in the observation area $\langle N_1 \rangle$. For $\langle N_1 \rangle \gg 1$, the values of $G_{m,n}(0)$ decay as $\langle N_1 \rangle^{-m}$ for $m = n = 1, 2$, or 3; and as $\langle N_1 \rangle^{-(m+1)}$ for $m \neq n$. (*b*) Shown are constant-value lines of $G_{1,1}(0)$, for a sample containing an average of 1,000 molecules in the observation area, with an average of $\langle N_1 \rangle$ monomers with relative fluorescence yield $\alpha_1 = 1$ and $\langle N_2 \rangle$ oligomers of p molecules with relative fluorescence yield $\alpha_2 = p$. As few as 25 dimers, eight trimers, or two hexamers change the value of $G_{1,1}(0)$ by 5%. More extensive clustering can increase the value of $G_{1,1}(0)$ by a factor greater than 100.

where

$$h(\mathbf{r}) = I(\mathbf{r})/I_0 \tag{21}$$

is the intensity profile normalized by its maximum value I_0, and constants h_n are defined as

$$h_n = \int h^n(\mathbf{r})\, d^2r / \int h(\mathbf{r})\, d^2r. \tag{22}$$

Table I shows the values of h_n for several common illumination and detection profiles $I(\mathbf{r})$. Using the values of h_n from Table I in Eqs. 20 shows that the values of $G_{m,n}(0)$ are higher for illumination profiles with sharp edges (i.e., not Gaussian-shaped). Although higher values of $G_{m,n}(0)$ are usually more readily measured against background noise, these illumination profiles may in practice be more difficult to use because the values of $G_{m,n}(0)$ can only be measured by extrapolating from non-zero times, since the experimental value of $G_{m,n}(0)$ contains a large component of shot noise, and the initial slope of $G_{m,n}(t)$ can be expected to be high for illumination profiles with sharp edges (Axelrod et al., 1976*b*).

Time-Dependence of High Order Fluorescence Fluctuation Autocorrelation Functions

The time dependence of the $G_{m,n}(t)$ has been calculated primarily to determine appropriate theoretical functional forms for fitting to experimentally obtained autocorrelation functions and to ensure that data have been obtained at times early enough to accurately extrapolate values of $G_{m,n}(0)$. As expected for a system in equilibrium, the time course of the autocorrelation functions given by Eq. 15 is symmetric upon an interchange of m and n. The time constant for the decay of $L_{m,n}(i, t)$ decreases as $2mn/(m+n)$, which means that higher order correlations have components that decay faster than lower order ones. Although in theory an infinite number of $G_{m,n}(t)$ can be calculated from experimental data, in practice only $G_{m,n}(t)$'s that decay slowly enough to be reliably extrapolated to time zero are useful. This limit depends on the relative sizes of the experimental counting interval and the time constants for the transport processes given in Eqs. 16.

TABLE I
VALUES OF CONSTANTS h_n FOR COMMON INTENSITY PROFILES $I(\mathbf{r})$

$I(\mathbf{r})$	h_n	Comments
$I_0 \exp(-2r^2/s^2)$	$1/n$	Focused TEM_{00} laser beam
$I_0 \exp(-2(x^2 + \gamma^2 y^2)/s^2)$	$1/n$	Totally internally reflected TEM_{00} laser beam
I_0 $\lvert x\rvert < s/2$, $\lvert y\rvert < \gamma s/2$	1	Rectangular image plane aperture
I_0 $r < s$	1	Circular image plane aperture

For a single species ($R = 1$), the relative contributions of the different terms to the $F_{m,n}(t)$ shown in Eqs. 14 and 15 depend on the value of $\langle N_1 \rangle$. For $\langle N_1 \rangle \ll 1$, the leading terms $L_{m,n}(i, t)$ dominate the remaining terms, and, in the absence of flow or sample translation ($V = 0$), each $F_{m,n}(t)$ is proportional to $\langle N_1 \rangle^{-(m+n-1)}$ and is a single Lorentzian with a half-time of $[(m + n)/(2mn)]\tau_{D_1}$. For $\langle N_1 \rangle \gg 1$, the Poisson distribution of number fluctuations becomes approximately Gaussian, the leading terms $L_{m,n}(i, t)$ are dominated by the remaining terms, and the $F_{m,n}(t)$'s are approximate functions of $F_{1,1}(t)$ and $F_{1,2}(t)$. Fig. 2 shows $F_{m,n}(t)$, normalized to a time-zero value of one, for $\langle N_1 \rangle = 50$ and $V = 0$.

Obtaining the Distribution of Particles with Different Relative Fluorescence Yields

As shown by Eqs. 17 and 18, for each value of $m + n$, one new quantity B_{m+n} can be determined from the measured value of $G_{m,n}(0)$; information on the average number of particles of different species in the illuminated area is obtained from the B_k's. The system of equations for the B_k's is made more tractable by the substitution

$$z = \sum_{i=1}^{R} \alpha_i \langle N_i \rangle \tag{23}$$

into Eq. 18 to give

$$z^k B_k = z + \sum_{i=2}^{R} \alpha_i(\alpha_i^{k-1} - 1)\langle N_i \rangle. \tag{24}$$

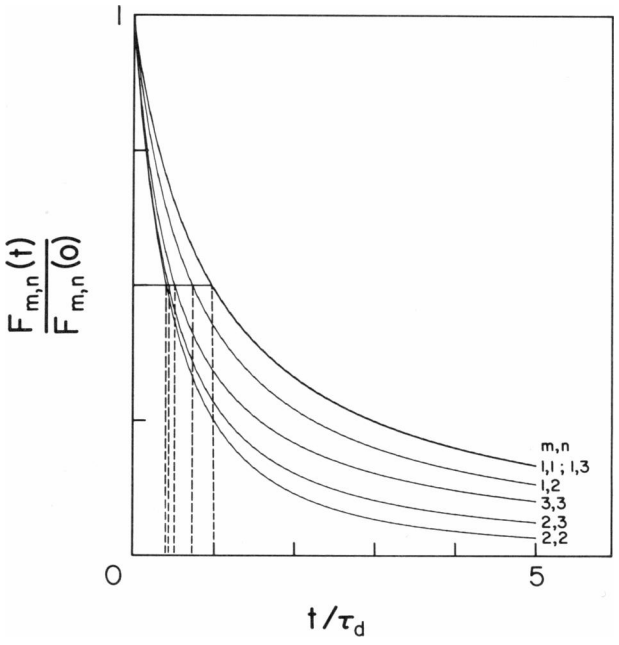

FIGURE 2 Theoretical time dependence of high order fluorescence fluctuation autocorrelation functions for a monodisperse sample with $\langle N_1 \rangle = 50$ and no sample translation ($V = 0$). The $F_{m,n}(t)$ decay as sums of Lorentzians and products of Lorentzians as given by Eqs. 14 and 15 with $V = 0$. The relative contribution of different terms depends on the value of $\langle N_1 \rangle$.

If the relative quantum efficiencies α_i are unknown, then the first species contributes one unknown ($\langle N_1 \rangle$) and each new species after the first contributes two unknowns ($\langle N_i \rangle$ and α_i, for the ith species). Thus, for a single species only B_2 must be calculated, and

$$\langle N_1 \rangle = 1/B_2 \quad (R = 1). \tag{25}$$

When two species are present, z, $\langle N_1 \rangle$, $\langle N_2 \rangle$, and α_2 may be determined from B_2, B_3, and B_4 by solving Eq. 24 with $k = 2$, 3, and 4, for z, $\langle N_2 \rangle$, and α_2 and then using Eq. 23 to find $\langle N_1 \rangle$. The results are

$$z = \{(B_4 - B_2B_3) \pm [(B_2B_3 - B_4)^2 - 4(B_2^2 - B_3)(B_3^2 - B_2B_4)]^{1/2}\}/ 2(B_3^2 - B_2B_4) \tag{26a}$$

$$\alpha_2 = (z^2B_3 - zB_2)/(zB_2 - 1) \tag{26b}$$

$$\langle N_2 \rangle = z(zB_2 - 1)/[\alpha_2(\alpha_2 - 1)] \tag{26c}$$

$$\langle N_1 \rangle = z - \alpha_2\langle N_2 \rangle \quad (R = 2). \tag{26d}$$

Choosing the positive or negative square root for z in Eq. 26a interchanges the results for $\langle N_1 \rangle$ and $\langle N_2 \rangle$.

When three species are present, $\langle N_i \rangle$ for $i = 1$ to 3 and α_i for $i = 2$ and 3, may be determined from the B_k's for $k =$ 2 to 6 by solving Eqs. 23 and 24 with $k = 2$ to 6. The results are that z is given by the roots of the cubic equation

$$\begin{aligned}(B_4^3 + B_2B_5^2 + B_3^2B_6 - B_2B_4B_6 - 2B_3B_4B_5) \quad & z^3 \\ + (B_4B_6 - B_2B_3B_6 - B_3B_4^2 + B_3^2B_5 + B_2B_4B_5 - B_5^2) \quad & z^2 \\ + (B_2^2B_6 - B_3B_6 + B_3^2B_4 - B_2B_4^2 + B_4B_5 - B_2B_3B_5) \quad & z \\ + (2B_2B_3B_4 + B_3B_5 - B_2^2B_5 - B_3^3 - B_4^2) = 0,\end{aligned} \tag{27}$$

and that the following equations sequentially provide values for α_2, α_3, $\langle N_2 \rangle$, $\langle N_3 \rangle$, and $\langle N_1 \rangle$:

$$\begin{aligned}C_1 &= [(zB_4 - B_3)^2 - (zB_3 - B_2)(zB_5 - B_4)]/ [(1 - zB_2)(zB_4 - B_3) + (zB_3 - B_2)^2] \\ C_2 &= [(1 - zB_2)(zB_5 - B_4) + (zB_3 - B_2)(zB_4 - B_3)]/ [(1 - zB_2)(zB_4 - B_3) + (zB_3 - B_2)^2] \\ C_3 &= [C_2 \pm (C_2^2 - 4C_1)^{1/2}]/2 \\ \alpha_2 &= zC_1/C_3 \\ \alpha_3 &= zC_3 \\ \langle N_2 \rangle &= [z\alpha_3(zB_2 - 1) - z^2(zB_3 - B_2)]/ [\alpha_2(\alpha_2 - 1)(\alpha_3 - \alpha_2)] \\ \langle N_3 \rangle &= [z\alpha_2(zB_2 - 1) - z^2(zB_3 - B_2)]/ [\alpha_3(\alpha_3 - 1)(\alpha_2 - \alpha_3)] \\ \langle N_1 \rangle &= z - \alpha_2\langle N_2 \rangle - \alpha_3\langle N_3 \rangle \quad (R = 3).\end{aligned} \tag{28}$$

The three roots of the cubic equation for z and the two roots of the quadratic equation for C_3 result in six solutions to the set of equations that correspond to the six permutations of the three species between $\langle N_1 \rangle$, $\langle N_2 \rangle$, and $\langle N_3 \rangle$.

In some experiments, the relative quantum efficiencies α_i may be known. In this case, each new species requires only one and not two new values of B_k. The variables in Eq. 24 are z and the $\langle N_i \rangle$'s and because the equations are linear in the $\langle N_i \rangle$'s, straightforward elimination of $R - 1$ $\langle N_i \rangle$'s from Eqs. 24 with $k = 2$ to $R + 1$ yields a polynomial of order R in z with coefficients that are functions of the B_k's and α_i's. Depending on the value of R, the polynomial may be solved analytically or numerically for z and then the $\langle N_i \rangle$'s may be determined by sequential substitution and use of Eq. 23.

EXPERIMENTAL METHODS

Optics and Electronics

The optical apparatus was similar to that used previously in microscope-based FCS (Magde et al., 1974; Thompson and Axelrod, 1983). The 514.5-nm line of an argon ion laser (Innova 90-3; Coherent Inc., Palo Alto, CA) was passed through auxiliary lenses into the epi-illumination port of an inverted optical microscope (Zeiss IM-35; Eastern Microscope Co., Raleigh, NC), reflected by a dichroic mirror (Omega Optical, Inc., Brattleboro, VT), and focused to a small spot on the sample through a 60×, 1.4 numerical aperture objective (Nikon Inc., Garden City, NY). The $1/e^2$ radius of the focused spot was visually judged to be $\lesssim 1$ μm, which was consistent with an estimate of >0.2 μm calculated from the geometry of the optical system and characteristics of the input beam (Wahl, 1985). Fluorescence originating from the sample was passed through a filter block and detected by a single-photon counting, thermoelectrically cooled photomultiplier (model 31034A; RCA, Lancaster, PA) coupled to the video port of the microscope. Fluorescence originating from outside of the sample volume was partially blocked by a 200-μm pinhole mounted in an intermediate focal plane of the microscope and positioned by an externally controlled x-y translation stage. The photomultiplier signal was passed through an amplifier/discriminator and then to a PC AT microcomputer (IBM Instruments, Inc., Danbury, CT), equipped with a pulse-counting interface board (Tecmar Labmaster Board; Arrow Electronics, Raleigh, NC). ASYST software (Macmillan Software Co., Macmillan Publishing Co., New York, NY) was used to count the number of photoelectron pulses p_j occurring between consecutive sample times $j\Delta T$ to $(j + 1)\Delta T$. The laser, microscope, and supporting optics were mounted on a vibration-isolated air table (Newport RS-46-8; Newport Corp., Fountain Valley, CA).

Sample Preparation and Data Collection

Freshly prepared solutions of 10^{-7} M diI in H_2O/ethyl alcohol (EtOH) at (4:1, vol/vol) or (1:1, vol/vol) were mounted on the microscope stage in 50-μm path-length glass microcapillary tubes (Vitro Dynamics Inc., Rockaway, NJ). Fluorescence was measured as the number of photoelectron pulses p_j occurring in ten records of 16,384 consecutive counting intervals with $\Delta T = 2$ ms, and stored on the IBM PC AT hard disk as single byte integers for off-line processing. Background intensity was measured from blank solutions of H_2O/EtOH. The laser power was 10 μW, samples were not translated through the beam, and all experiments were done at room temperature. The average fluorescence intensity of each sample was constant for the duration of the experiment.

Autocorrelation Software, Background Corrections, and Data Analysis

Each fluorescence record was processed off-line to give $H_{m,n}(i\Delta T)$ according to the following algorithm:

$$H_{m,n}(i\Delta T) = \langle p\rangle^{-(m+n)}(15{,}104\,M)^{-1} \cdot \sum_{q=1}^{M}\sum_{j=1,281}^{16,384}[(p_{q,j-i} - \langle p\rangle)^n(p_{q,j} - \langle p\rangle)^m - (p_{q,j-k} - \langle p\rangle)^n(p_{q,j} - \langle p\rangle)^m], \quad (29)$$

where $p_{q,j}$ was the number of photoelectron pulses in the jth interval of the qth record, k was cyclically varied between 1,280 and 1,153 to eliminate long-time correlations between $p_{q,j+k}$ and $p_{q,j}$, $M = 10$ was the number of data records, i was an integer between 0 and 128, and

$$\langle p\rangle = (16{,}384\,M)^{-1}\sum_{q=1}^{M}\sum_{j=1}^{16,384} p_{q,j}. \quad (30)$$

The algorithm uses the relation that $G_{m,n}(t) = G_{n,m}(-t)$ for an arbitrary signal (Steinberg, 1986). Typical times for calculating $H_{m,n}(i\Delta T)$ for one set of m,n values on an IBM PC AT equipped with a math coprocessor were 4 h with ASYST and 1 h with IBM Pro Fortran.

For low fluorescent photon count rates, the background intensity was a non-negligible fraction of the measured fluorescence. The calculated $H_{m,n}(i\Delta T)$ were corrected for background fluorescence using a generalization of previous methods (Thompson and Axelrod, 1983; Icenogle and Elson, 1983*a*). If the number of photoelectron pulses per sample time arising from fluorophores is $p_f(t)$ and arising from the background is $p_b(t)$, then the autocorrelation function $H_{m,n}(i\Delta T)$ calculated from data is

$$\begin{aligned} H_{m,n}(i\Delta T) &= \{\langle[\delta p_f(t + i\Delta T) + \delta p_b(t + i\Delta T)]^m[\delta p_f(t) + \delta p_b(t)]^n\rangle \\ &\quad - \langle[\delta p_f(t) + \delta p_b(t)]^m\rangle\langle[\delta p_f(t) + \delta p_b(t)]^n\rangle\}/ \\ &\quad \langle p_f(t) + p_b(t)\rangle^{m+n} \\ &= \sum_{i=0}^{m-1}\sum_{j=0}^{n-1}\binom{m}{i}\binom{n}{j}\langle\delta p_b^i\rangle\langle\delta p_b^j\rangle\langle p_f\rangle^{m+n-i-j} \\ &\quad \cdot G_{m-i,n-j}(i\Delta T)/[\langle p_f\rangle + \langle p_b\rangle]^{m+n}, \end{aligned} \quad (31)$$

where

$$\delta p_{f,b}(t) = p_{f,b}(t) - \langle p_{f,b}\rangle, \quad (32)$$

and $\binom{m}{i}$ are binomial coefficients. The assumptions have been made that fluctuations in fluorophore fluorescence are not correlated with fluctuations in background intensity and that fluctuations in background intensity are correlated only at times much shorter than ΔT. Thus,

$$G_{m,n}(i\Delta T) = \kappa^{m+n}H_{m,n}(i\Delta T) \quad \text{for } (n, m) = (1, 1), (1, 2), (2, 1), (2, 2) \quad (33a)$$

$$G_{m,3}(i\Delta T) = \kappa^{m+3}H_{n,3}(i\Delta T) - 3G_{m,1}(i\Delta T)\langle p_b\rangle/\langle p_f\rangle^2 \text{ for } m = 1, 2 \quad (33b)$$

$$G_{3,n}(i\Delta T) = \kappa^{n+3}H_{3,n}(i\Delta T) - 3G_{1,n}(i\Delta T)\langle p_b\rangle/\langle p_f\rangle^2 \text{ for } n = 1, 2 \quad (33c)$$

$$G_{3,3}(i\Delta T) = \kappa^6 H_{3,3}(i\Delta T) - 3\langle p_b\rangle/\langle p_f\rangle^2[G_{1,3}(i\Delta T) + G_{3,1}(i\Delta T)] - [3\langle p_b\rangle/\langle p_f\rangle^2]^2 G_{1,1}(i\Delta T), \quad (33d)$$

where

$$\kappa = (\langle p_f\rangle + \langle p_b\rangle)/\langle p_f\rangle, \quad (34)$$

$\langle\delta p_f\rangle = \langle\delta p_b\rangle = 0$, and $\langle\delta p_b^i\rangle$ are assumed to be the ith moments about the mean of a Poisson distribution given in Eqs. B12.

Nine autocorrelation functions, corresponding to the possible combinations of $1 \le m,n \le 3$ and m not necessarily less than n, were calculated from each set of ten fluorescence records. The $G_{m,n}(0)$ calculated by Eqs. 31 and 33 contains a large component of shot noise; therefore, the time-zero values are determined by extrapolation from the autocorrelation functions at longer times. The background-corrected autocorrelation functions were fit to theoretical forms using the iterative Gauss–Newton nonlinear curve-fitting routine in ASYST. Theoretical functional forms were either the single species functions given by Eqs. 14 and 15 with $V = 0$ and modified by addition of a constant term, or single Lorentzians modified by addition of a constant term. All functional forms had three free parameters and fits were considered optimized when the free parameters were stable to three significant figures. The values of the B_k's were determined from the extrapolated time-zero quantities $G_{m,n}(0)$ according to the following adaption of Eqs. 17:

$$\begin{aligned} B_2 &= G_{1,1}(0) \\ B_3 &= (3/8)[G_{1,2}(0) + G_{2,1}(0)] \\ B_4 &= (1/6)[G_{2,2}(0) + G_{1,3}(0) + G_{3,1}(0) - 8B_2^2] \\ B_5 &= (5/32)[G_{2,3}(0) + G_{3,2}(0) - 24B_2B_3] \\ B_6 &= (3/16)[G_{3,3}(0) - 30B_2B_4 - 15B_2^3 - 16B_3^2]. \end{aligned} \quad (35)$$

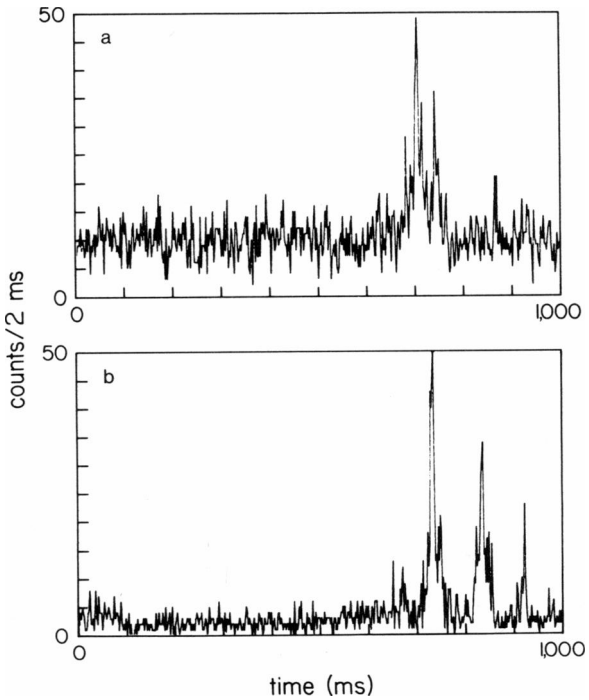

FIGURE 3 Sections of the experimentally measured fluorescence for 10^{-7} M dil in H_2O/EtOH at (*a*) (1:1) and (*b*) (4:1). Both samples display occasional large fluctuations in measured and visually observed fluorescence.

EXPERIMENTAL RESULTS

The background-corrected average measured fluorescence values for dil in H_2O/EtOH (4:1) and (1:1) were 720 ± 125 counts/s and 3,800 ± 600 counts/s, respectively; the average background intensity was 250 ± 25 counts/s. One second segments of typical fluorescence records for dil in the two solutions are shown in Fig. 3. The occasional large fluorescence fluctuations present in the recorded fluorescence from the samples were also visible through the microscope.

Examples of background-corrected high order autocorrelation functions calculated from experimental data are shown in Figs. 4 and 5. Autocorrelation functions calculated for the blank samples did not show correlations for times greater than the sample time $\Delta T = 2$ ms.

Also shown in Figs. 4 and 5 are examples of best fits of experimental autocorrelation functions to the single species functions given by Eqs. 14 and 15 with $V = 0$, and modified by addition of a constant term, for the two H_2O/EtOH solutions. The average extrapolated time-zero values $G_{m,n}(0)$ are given in Table II. The average values of τ_D obtained from the best fits were 9.2 ± 1.0 ms (4:1) and 9.6 ± 1.6 ms (1:1).

The extrapolated time-zero values $G_{m,n}(0)$ of autocorrelation functions for different samples with the same water content were variable, but sets of $G_{m,n}(0)$'s appeared to systematically vary from one sample to another. Accordingly, the values of the B_k's and subsequently the $\langle N_i \rangle$'s and α_i's were calculated separately from the set of $G_{m,n}(0)$ values from each fluorescence record rather than from the average time-zero results shown in Table II. Each set of B_k values was analyzed assuming that one, two, or three species was present as described in an above theoretical section (Eqs. 23–28). The average results for $\langle N_1 \rangle$, $\langle N_2 \rangle$, $\langle N_3 \rangle$, α_2, and α_3 under the different assumed distributions are given in Table III.

The data were also fit with single Lorentzian functions having three parameters: intercept, time constant, and

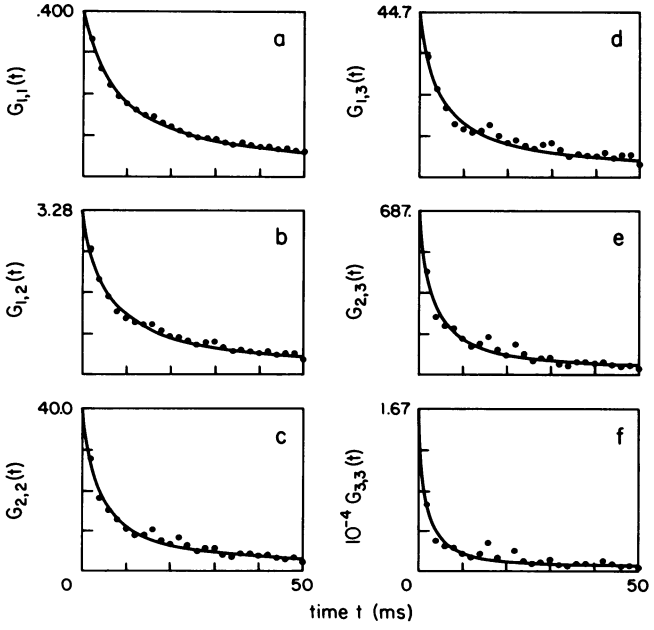

FIGURE 4 Experimental high order fluorescence fluctuation autocorrelation functions and theoretical best fits for 10^{-7} M dil in H_2O/EtOH (4:1). The experimental functions (*a*) $G_{1,1}(t)$, (*b*) $G_{1,2}(t)$, (*c*) $G_{2,2}(t)$, (*d*) $G_{1,3}(t)$, (*e*) $G_{2,3}(t)$, and (*f*) $G_{3,3}(t)$ calculated from a single fluorescence record of 163,840 points and their best fits to the monodisperse functions $F_{m,n}(t)$ given by Eqs. 14 are shown.

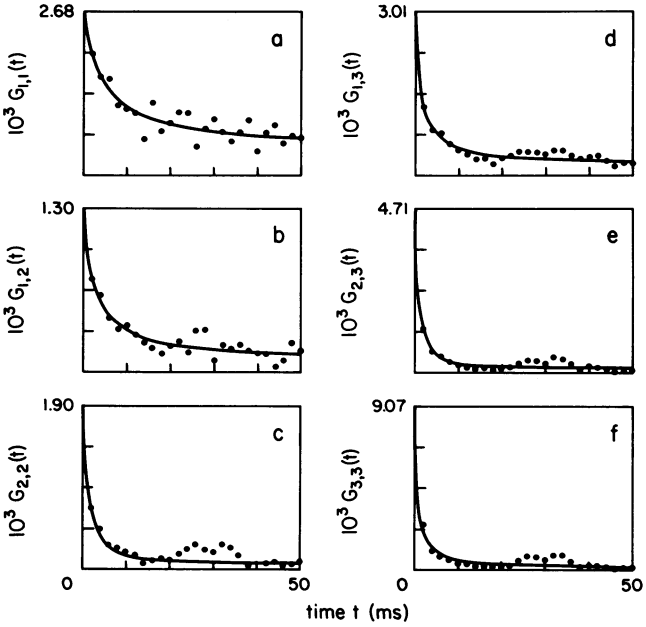

FIGURE 5 Experimental high order fluorescence fluctuation autocorrelation functions and theoretical best fits for 10^{-7} M dil in H_2O/EtOH (1:1). The experimental functions (*a*) $G_{1,1}(t)$, (*b*) $G_{1,2}(t)$, (*c*) $G_{2,2}(t)$, (*d*) $G_{1,3}(t)$, (*e*) $G_{2,3}(t)$, and (*f*) $G_{3,3}(t)$ calculated from a single fluorescence record of 163,840 points and their best fits to the monodisperse functions $F_{m,n}(t)$ given by Eqs. 14 are shown.

TABLE II
EXTRAPOLATED TIME-ZERO VALUES OF HIGH ORDER FLUORESCENCE FLUCTUATION AUTOCORRELATION FUNCTIONS FOR dil SUSPENDED IN WATER/ETHANOL SOLUTIONS

	H_2O/EtOH (4:1)	H_2O/EtOH (1:1)
$G_{1,1}(0)$	2.3 ± 0.8	$(9.0 \pm 1.8) \times 10^{-3}$
$G_{1,2}(0)$	111 ± 54	$(3.3 \pm 1.7) \times 10^{-2}$
$G_{2,1}(0)$	115 ± 56	$(3.4 \pm 1.8) \times 10^{-2}$
$G_{2,2}(0)$	$(1.6 \pm 0.8) \times 10^4$	0.33 ± 0.18
$G_{1,3}(0)$	$(1.2 \pm 0.6) \times 10^4$	0.30 ± 0.20
$G_{3,1}(0)$	$(1.0 \pm 0.5) \times 10^4$	0.32 ± 0.21
$G_{2,3}(0)$	$(1.6 \pm 0.6) \times 10^6$	2.9 ± 2.2
$G_{3,2}(0)$	$(1.1 \pm 0.8) \times 10^6$	3.7 ± 2.3
$G_{3,3}(0)$	$(2.4 \pm 1.4) \times 10^8$	40 ± 27

Shown are the average extrapolated values of $G_{m,n}(0)$ and the standard errors of the means from 13 (or 12) and 11 (or 10) samples of dil in H_2O/EtOH 4:1 and 1:1, respectively. $G_{2,3}(t)$, $G_{3,2}(t)$, and $G_{3,3}(t)$ for one sample of each type could not be fit to theoretical functional forms and were excluded from the averages.

TABLE III
NUMBER DENSITIES AND RELATIVE FLUORESCENCE YIELDS OF dil AGGREGATES IN WATER/ETHANOL SOLUTIONS

	H_2O/EtOH (4:1)	H_2O/EtOH (1:1)
One species		
$\langle N_1 \rangle$	1.1 ± 0.3	180 ± 40
Two species		
$\langle N_1 \rangle$	3.1 ± 1.0	360 ± 50
$\langle N_2 \rangle$	$(1.1 \pm 0.3) \times 10^{-3}$	$(6.3 \pm 0.2) \times 10^{-4}$
α_2	110 ± 30	$(1.2 \pm 0.3) \times 10^3$
Three species		
$\langle N_1 \rangle$	2.3 ± 1.0	360 ± 60
$\langle N_2 \rangle$	$(1.1 \pm 0.4) \times 10^{-3}$	$(7 \pm 2) \times 10^{-4}$
α_2	100 ± 30	900 ± 20
$\langle N_3 \rangle$	$(-9 \pm 9) \times 10^{-5}$	$(-1.6 \pm 1.5) \times 10^{-4}$
α_3	$(-1.7 \pm 1.7) \times 10^3$	700 ± 1,200

Shown are the averages and standard errors of the means of the number densities and relative fluorescence yields of dil aggregates in H_2O/EtOH, 4:1 and 1:1, assuming that one, two, or three aggregate species are present. Averages for the one and two species analyses are calculated from 13 or 11 samples of the 4:1 or 1:1 solutions, respectively. The $G_{2,3}(t)$, $G_{3,2}(t)$, and $G_{3,3}(t)$ functions for one of the 4:1 samples and one of the 1:1 samples could not be fit to trial functions, and three of the 4:1 samples and one of the 1:1 samples gave negative values for $\langle N_1 \rangle$, α_2, and α_3. These samples were excluded from the reported results of the three species analyses.

additive constant (data not shown). Although the single species functions fit the time course of the data better for $m + n > 3$ and the Lorentzian functions resulted in extrapolated time-zero values that were systematically lower, the average calculated distributions from the two fitting procedures were not significantly different.

Fig. 6 shows the close agreement between a typical high order autocorrelation function $G_{1,3}(t)$ and its time-reverse function $G_{3,1}(t)$, as expected for a system in equilibrium (Steinberg, 1986).

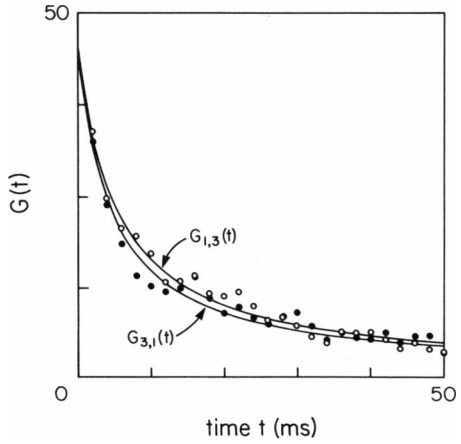

FIGURE 6 Comparison of the experimental values and theoretical best fits for $G_{1,3}(t)$ (O) and $G_{3,1}(t)$ (●) for 10^{-7} M dil in H_2O/EtOH (4:1). The experimental curves are identical within experimental uncertainty.

DISCUSSION

This paper describes the theoretical dependence of extrapolated time-zero values of high order fluorescence fluctuation autocorrelation functions in FCS on the number densities and fluorescence yields of different fluorescent species, the theoretical time dependence of the high order autocorrelation functions on transport coefficients, and the first experimental application of the use of high order autocorrelation functions in FCS to characterize aggregation of the fluorescent lipid dil in solutions of water and ethyl alcohol.

For dil in both 4:1 and 1:1 H_2O/EtOH, the sets of time-zero values of high order fluorescence fluctuation autocorrelation functions shown in Table II are not consistent with those expected for monodisperse samples. In addition, the two dil suspensions have different average values of fluorescence and different autocorrelation function time-zero values, which suggest that the suspensions have different dispersions. As shown in Table III, assuming a monodisperse sample indicates that, as found earlier (Koppel et al., 1976), the sample with more water has fewer, and presumably larger, aggregates. However, assuming that the samples contain two different fluorescent species indicates the presence of one predominant species and a very low concentration of another species with a large fluorescence yield relative to that of the predominant species. If the two species analysis has correctly identified the presence of large aggregates in the samples, then the large aggregates cause the monodisperse analysis to underestimate the concentration of the predominant species by a factor of two to three. The differences between the average numbers of particles of the predominant species ($\langle N_1 \rangle$), shown in Table II, for the monodisperse analyses and the two-species analyses are significant at $P = 0.01$ for the 4:1 sample and $P = 0.001$ for the 1:1 sample using a paired t test (Devore, 1982). The values for the average number of large aggregates ($\langle N_2 \rangle$) and the relative fluorescence yield of the large aggregates (α_2) for both samples are significantly greater than zero at $P = 0.005$ using a t test.

The dimensions of the open volume defined by the laser beam in the experimental apparatus used have not been measured so the absolute concentration of the species in the samples is unknown. Assuming that the beam's $1/e^2$-radius is no larger than 1 μm, and that fluorescence is collected from a maximum depth of 50 μm (the path length of the microslide), then the upper limit for the sample volume is 50 μm^3. The maximum volume, the known concentration of dil in the samples, and the results for $\langle N_1 \rangle$ from the two-species analysis imply that the predominant species in the 1:1 sample is at most an octamer of dil molecules.

As shown in Table II, the values of $G_{m,n}(0)$ dramatically increase with increasing $m + n$, in contrast to the expected decrease in $G_{m,n}(0)$ for a monodisperse sample with $\langle N_1 \rangle > 1$. This occurs because $\alpha_2^{m+n} \langle N_2 \rangle \gg \langle N_1 \rangle >$

$\alpha_2\langle N_2\rangle$ for $m + n > 2$, and, referring to Eqs. 17 and 18, $B_{m+n} \simeq \langle N_2\rangle(\alpha_2/\langle N_1\rangle)^{m+n}$. In the two diI solutions $\alpha_2/\langle N_1\rangle > 1$; therefore, $G_{m,n}(0)$ increases with $m+n$. The marked effect of the large aggregates on the high order autocorrelation functions was the reason that the single-species functions were used for extrapolating the time-zero values.

The calculated low concentration of large aggregates is consistent with the observed frequency of the occasional large fluorescence fluctuations shown in Fig. 3. Typically, only a few hundred of the 163,840 counting intervals per fluorescence record contained such large fluorescence fluctuations, which suggests that uncertainty in the values of $G_{m,n}(0)$ shown in Table II is a consequence of differences in sampling the concentration of large aggregates between individual fluorescence records. In addition, because relatively few characteristic fluctuations of the large aggregates were recorded, the high order autocorrelation functions dominated by the large aggregates tended to contain more noise. As a result, a detailed analysis of the time course of the experimental autocorrelation functions was not undertaken.

The three-species analysis of the two samples, after excluding a few of the fluorescence records, implies values for $\langle N_1\rangle$, $\langle N_2\rangle$, and α_2 that are consistent with the two-species analysis and values for $\langle N_3\rangle$ and α_3 that are not significantly different from zero, as shown in Table III.

Since the leading term in the single species functions given by Eqs. 14 and 15 decreases as $\langle N_1\rangle^{m+n-1}$, other generalized autocorrelation functions might be sought that would be less strongly dependent on $\langle N_1\rangle$. For example, the definition in Eq. 2 can be extended to include powers a and b which are real but not integral. Expanding the quantity $\langle F^a(t+\tau)F^b(t)\rangle$ in a binomial series gives

$$\begin{aligned}\langle F^a(t+\tau)F^b(t)\rangle &= \langle [\langle F(t+\tau)\rangle \\ &\quad + \delta F(t+\tau)]^a[\langle F(t)\rangle + \delta F(t)]^b\rangle \\ &= \sum_{j=0}^{\infty}\sum_{k=0}^{\infty}\binom{a}{j}\binom{b}{k}\langle F(t)\rangle^{a+b-j-k} \\ &\quad \cdot \langle \delta F^j(t+\tau)\delta F^k(t)\rangle, \end{aligned} \tag{36}$$

where the fluorescence fluctuations are assumed to be small, i.e., that $\delta F^2 < \langle F\rangle^2$. Since j and k are integers, autocorrelation functions of non-integer order constructed from functions of the form in Eq. 36 are linear combinations of the values of $G_{m,n}(t)$ calculated in the above sections. Similarly, autocorrelation functions defined using any functional form that can be expanded in powers will also be linear combinations of the $G_{m,n}(t)$ defined in Eq. 2 (Steinberg, 1986).

Although the derivation of the $G_{m,n}(t)$ presented above does not include chemical reaction kinetics, the results obtained for $G_{m,n}(0)$ and B_k are nonetheless applicable to systems in which reversible reactions occur because the $G_{m,n}(0)$ values depend only on the Poisson nature of the number fluctuations in the sample. The time dependence of high order fluorescence fluctuation autocorrelation functions will depend in a complex manner on the chemical kinetic processes occurring in a sample and on the relative rates of the chemical and transport processes. In an experiment data must be collected faster than fluctuations decay due to these processes. In principle, the time dependence of the high order autocorrelation functions could be determined by generalizing the above derivation to include the more complex probability distribution functions that have been derived for reacting molecules (Aragón and Pecora, 1976).

Although the use of high order autocorrelation functions in FCS to determine the distribution of aggregate sizes has not yet been tested on a sample with a well-defined aggregate distribution, the experimental results for diI aggregation suggest that this method can provide the concentrations and the relative fluorescent yields of at least two fluorescent species in a sample. If the relative fluorescence yields of the species present in the sample can be independently measured, e.g., if the fluorescence yields are known to be proportional to the number of monomers per aggregate, then determination of the concentration of aggregates of different sizes could be expected to be even more feasible. Finally, the technique described in this paper should prove useful in accounting for the demonstrated large effect of aggregates in FCS, even in experiments not designed to investigate aggregation phenomena.

APPENDIX A

Derivation of the Multiple Species Concentration Fluctuation Correlation Functions $g_{m,n}$ in Terms of the Single Species Concentration Fluctuation Correlation Functions $f_{m,n}$

Under the assumption of a nonreactive, ideal solution, concentration fluctuations from two different chemical species are not correlated, so that the functions $g_{m,n}(i_1, i_2, \cdots i_{m+n}; \mathbf{r}_1, \mathbf{r}_2, \cdots, \mathbf{r}_{m+n}; t)$ can be written as sums of products of Kronecker deltas and single species concentration fluctuation correlation functions. For example,

$$\begin{aligned} g_{1,1}(i, j, \mathbf{r}_1, \mathbf{r}_2; t) &= \delta_{ij}[\langle \delta C_i(\mathbf{r}_1, t)\delta C_i(\mathbf{r}_2, 0)\rangle \\ &\quad - \langle \delta C_i(\mathbf{r}_1, t)\rangle\langle \delta C_i(\mathbf{r}_2, t)\rangle] \\ &\quad + (1 - \delta_{ij})[\langle \delta C_i(\mathbf{r}_1, t)\rangle\langle \delta C_j(\mathbf{r}_2, 0)\rangle \\ &\quad - \langle \delta C_i(\mathbf{r}_1, t)\rangle\langle \delta C_j(\mathbf{r}_2, t)\rangle], \end{aligned} \tag{A1}$$

where δ_{ij} is the Kronecker delta. In addition, the ensemble average of concentration fluctuations in each ith species is zero:

$$\langle \delta C_i(\mathbf{r}, t)\rangle = 0\,. \tag{A2}$$

Writing expressions similar to Eq. A1 for a given $g_{m,n}$, and using Eq. A2

gives

$$g_{1,1}(i, j; r_1, r_2; t) = \delta_{ij} f_{1,1}(i, r_1, r_2; t);$$

$$g_{1,2}(i, j, k; r_1, r_2, r_3; t) = \delta_{ij}\delta_{ik} f_{1,2}(i, r_1, r_2, r_3; t);$$

$$\begin{aligned} g_{2,2}&(i, j, k, l; r_1, r_2, r_3, r_4; t) \\ &= \delta_{ij}\delta_{ik}\delta_{il}\langle \delta C_i(r_1, t)\delta C_i(r_2, t)\delta C_i(r_3, 0)\delta C_i(r_4, 0)\rangle \\ &\quad + (1 - \delta_{ik})\delta_{ij}\delta_{kl}\langle \delta C_i(r_1, t)\delta C_i(r_2, t)\rangle \langle \delta C_k(r_3, 0)\delta C_k(r_4, 0)\rangle \\ &\quad + (1 - \delta_{ij})\delta_{ik}\delta_{jl}\langle \delta C_i(r_1, t)\delta C_i(r_3, 0)\rangle \langle \delta C_j(r_2, t)\delta C_j(r_4, 0)\rangle \\ &\quad + (1 - \delta_{ij})\delta_{il}\delta_{jk}\langle \delta C_i(r_1, t)\delta C_i(r_4, 0)\rangle \langle \delta C_j(r_2, t)\delta C_j(r_3, 0)\rangle \\ &\quad - \delta_{ij}\delta_{kl}\langle \delta C_i(r_1, t)\delta C_i(r_2, t)\rangle \langle \delta C_k(r_3, 0)\delta C_k(r_4, 0)\rangle. \end{aligned} \quad \text{(A3a)}$$

Above, the factors like $(1 - \delta_{ij})$ ensure that the case in which i, j, k, and l are all equal is not counted more than once, and the last term arises from the second term in Eq. 6. Thus,

$$\begin{aligned} g_{2,2}&(i, j, k, l; r_1, r_2, r_3, r_4; t) \\ &= \delta_{ij}\delta_{ik}\delta_{il} f_{2,2}(i; r_1, r_2, r_3, r_4; t) \\ &\quad + (1 - \delta_{ij})\delta_{ik}\delta_{jl} f_{1,1}(i, r_1, r_3; t) f_{1,1}(j, r_2, r_4; t) \\ &\quad + (1 - \delta_{ij})\delta_{il}\delta_{jk} f_{1,1}(i, r_1, r_4; t) f_{1,1}(j, r_2, r_3; t). \end{aligned} \quad \text{(A3b)}$$

Similar reasoning yields

$$\begin{aligned} g_{1,3}&(i, j, k, l; r_1, r_2, r_3, r_4; t) \\ &= \delta_{ij}\delta_{ik}\delta_{il} f_{1,3}(i; r_1, r_2, r_3, r_4; t) \\ &\quad + (1 - \delta_{ik})\delta_{ij}\delta_{kl} f_{1,1}(i, r_1, r_2; t) f_{1,1}(k, r_3, r_4; 0) \\ &\quad + (1 - \delta_{ij})\delta_{ik}\delta_{jl} f_{1,1}(i, r_1, r_3; t) f_{1,1}(j, r_2, r_4; 0) \\ &\quad + (1 - \delta_{ij})\delta_{il}\delta_{jk} f_{1,1}(i, r_1, r_4; t) f_{1,1}(j, r_2, r_3; 0); \end{aligned}$$

$$\begin{aligned} g_{2,3}&(i, j, \ldots, m; r_1, r_2, \ldots, r_5; t) \\ &= \delta_{ij}\delta_{ik}\delta_{il}\delta_{im} f_{2,3}(i; r_1, r_2, \ldots, r_5; t) \\ &\quad + (1 - \delta_{il})\delta_{ij}\delta_{ik}\delta_{lm} f_{1,2}(i, r_3, r_1, r_2; t) f_{1,1}(l, r_4, r_5; 0) \\ &\qquad \text{and two similar terms} \\ &\quad + (1 - \delta_{ij})\delta_{ik}\delta_{il}\delta_{jm} f_{1,2}(j, r_1, r_3, r_4; t) f_{1,1}(i, r_2, r_5; t) \\ &\qquad \text{and five similar terms;} \end{aligned}$$

$$\begin{aligned} g_{3,3}&(i, j, \ldots, n; r_1, r_2, \ldots, r_6; t) \\ &= \delta_{ij}\delta_{ik}\delta_{il}\delta_{im}\delta_{in} f_{3,3}(i; r_1, r_2, \ldots, r_6; t) \\ &\quad + (1 - \delta_{ij})\delta_{il}\delta_{im}\delta_{in}\delta_{jk} f_{1,3}(i, r_1, r_4, r_5, r_6; t) f_{1,1}(j, r_2, r_3; 0) \\ &\qquad \text{and five similar terms} \\ &\quad + (1 - \delta_{ik})\delta_{ij}\delta_{il}\delta_{im}\delta_{kn} f_{2,2}(i, r_1, r_2, r_4, r_5; t) f_{1,1}(k, r_3, r_6; t) \\ &\qquad \text{and eight similar terms} \\ &\quad + (1 - \delta_{ik})\delta_{ij}\delta_{il}\delta_{km}\delta_{kn} f_{1,2}(i, r_4, r_1, r_2; t) f_{1,2}(k, r_3, r_5, r_6; t); \\ &\qquad \text{and eight similar terms} \\ &\quad + (1 - \delta_{ik})(1 - \delta_{km})\delta_{ij}\delta_{kl}\delta_{mn} f_{1,1}(i, r_1, r_2; 0) \\ &\quad \cdot f_{1,1}(k, r_3, r_4; t) f_{1,1}(m, r_5, r_6; 0) \end{aligned}$$

$$\begin{aligned} &\text{and eight similar terms} \\ &+ (1 - \delta_{ij})(1 - \delta_{ik})(1 - \delta_{jk})\delta_{il}\delta_{jm}\delta_{kn} f_{1,1}(i, r_1, r_4; t) \\ &\cdot f_{1,1}(j, r_2, r_5; t) f_{1,1}(k, r_3, r_6; t) \\ &\text{and five similar terms.} \end{aligned} \quad \text{(A3c)}$$

The notation "similar term" refers to a different combination of species and their corresponding positions that gives rise to an identical integrated term in Eqs. 4 and 8. For example, in the second line of the above expression for $g_{2,3}$, the two "similar" terms are $(1 - \delta_{ik})\delta_{ij}\delta_{lm}\delta_{kl} f_{1,2}(i, r_5, r_1, r_2; t) f_{1,1}(k, r_3, r_4; 0)$ and $(1 - \delta_{ik})\delta_{ij}\delta_{il}\delta_{km} f_{1,2}(i, r_4, r_1, r_2; t) f_{1,1}(k, r_3, r_5; 0)$. Also, in deriving Eqs. A3, since only systems which are stationary in time are considered, $\langle \delta C_i(r_1, 0)\delta C_i(r_2, 0) \ldots \delta C_i(r_n, 0)\rangle = \langle \delta C_i(r_1, t)\, \delta C_i(r_2, t) \ldots \delta C(r_n, t)\rangle$.

APPENDIX B

Derivation of the Single Species Concentration Fluctuation Correlation Functions $f_{m,n}$

The (m, n) th-order correlation function of the concentration $C_i(r, t)$ of a given chemical species at positions $r_1, r_2, \ldots, r_m$ at time t with the concentration at positions $r_{m+1}, r_{m+2}, \ldots, r_{m+n}$ at time zero, is denoted by

$$\begin{aligned} S_{m,n}&(i, r_1, r_2, \ldots, r_{m+n}; t) = \langle C_i(r_1, t)C_i(r_2, t) \ldots \\ &C_i(r_m, t)C_i(r_{m+1}, 0)C_i(r_{m+2}, 0) \ldots C_i(r_{m+n}, 0)\rangle. \end{aligned} \quad \text{(B1)}$$

The concentration correlation functions can be determined by generalizing a derivation of $G_{1,1}(t)$ in terms of molecular correlation functions (Aragón and Pecora, 1976). Each molecule is a point source of concentration, so that

$$C_i(r, t) = \sum_{i'=1}^{I} \delta[r - r_{ii'}(t)], \quad \text{(B2)}$$

where $\delta[]$ is the Dirac delta function, $r_{ii'}(t)$ is the position of the i'th molecule of the ith-type species at time t, I is the number of molecules of the ith type in the sample, and the average number density of the ith species in the sample of closed area A is

$$\langle C_i\rangle = (1/A)\int_A C_i(r, t)\, \mathrm{d}^2 r = I/A. \quad \text{(B3)}$$

Using Eq. B2 in Eq. B1 gives

$$\begin{aligned} S_{m,n}&(i, r_1, r_2, \ldots, r_{m+n}; t) = \sum_{i_1=1}^{I}\sum_{i_2=1}^{I} \cdots \sum_{i_{m+n}=1}^{I} \\ &\langle \delta[r_1 - r_{ii_1}(t)] \ldots \delta[r_m - r_{ii_m}(t)] \\ &\cdot \delta[r_{m+1} - r_{ii_{m+1}}(0)] \ldots \delta[r_{m+n} - r_{ii_{m+n}}(0)]\rangle. \end{aligned} \quad \text{(B4)}$$

The position r'_{ii} of a given molecule is not correlated with the position $r_{ij'}$ of a different molecule. This means that the functions $S_{m,n}(i, r_1, r_2, \ldots r_{m+n}; t)$ can be written as sums of products of ensemble averages of sums of Dirac delta functions for the positions of single molecules. For example,

$$\begin{aligned} S_{1,1}&(i, r_1, r_2; t) = \sum_{j=1}^{I} \langle \delta[r_1 - r_{ij}(t)]\delta[r_2 - r_{ij}(0)]\rangle \\ &+ \sum_{\substack{j=1 \\ j\neq k}}^{I}\sum_{k=1}^{I} \langle \delta[r_1 - r_{ij}(t)]\rangle \langle \delta[r_2 - r_{ik}(0)]\rangle. \end{aligned} \quad \text{(B5)}$$

Assuming that the total number of molecules I of each ith species in the sample (not the average number of molecules in a small observed area) is large, then, referring to Eq. B2,

$$\sum_{i_1=1}^{I}\sum_{i_2=1}^{I}\cdots\sum_{i_{m+n-1}}^{I}\langle\delta[r_1-r_{ii_1}(t)]\rangle\langle\delta[r_2-r_{ii_2}(t)]\rangle\cdots$$

(no two indices equal)

$$\begin{aligned}&\langle\delta[r_m-r_{ii_m}(t)]\rangle\langle\delta[r_{m+1}-r_{ii_{m+1}}(0)]\rangle\\&\cdot\langle\delta[r_{m+2}-r_{ii_{m+2}}(0)]\rangle\langle\delta[r_{m+n}-r_{ii_{m+n}}(0)]\rangle\\&\simeq\langle C_i\rangle^{m+n}.\end{aligned}\tag{B6}$$

Using Eq. B6, along with the identities

$$\begin{aligned}&\sum_{j=1}^{I}\langle\delta[r_1-r_{ij}(t)]\delta[r_2-r_{ij}(t)]\ldots\delta[r_m-r_{ij}(t)]\rangle\\&=\sum_{j=1}^{I}\langle\delta[r_1-r_{ij}(0)]\delta[r_2-r_{ij}(0)]\ldots\delta[r_m-r_{ij}(0)]\rangle\\&=\delta(r_1-r_2)\delta(r_1-r_3)\ldots\delta(r_1-r_m)\sum_{j=1}^{I}\langle\delta[r_1-r_{ij}(0)]\rangle\\&=\langle C_i\rangle\delta(r_1-r_2)\delta(r_1-r_3)\ldots\delta(r_1-r_m),\end{aligned}\tag{B7}$$

and

$$\begin{aligned}&\sum_{j=1}^{I}\langle\delta[r_1-r_{ij}(t)]\delta[r_2-r_{ij}(t)]\ldots\delta[r_m-r_{ij}(t)]\\&\cdot\delta[r_{m+1}-r_{ij}(0)]\delta[r_{m+2}-r_{ij}(0)]\ldots\delta[r_{m+n}-r_{ij}(0)]\rangle\\&=\delta(r_1-r_2)\ldots\delta(r_1-r_m)\delta(r_{m+1}-r_{m+2})\ldots\delta(r_{m+1}-r_{m+n})\\&\cdot\sum_{j=1}^{I}\langle\delta[r_1-r_{ij}(t)]\delta[r_{m+1}-r_{ij}(0)]\rangle,\end{aligned}\tag{B8}$$

and the definition

$$P(i,r_1,r_2,t)=\sum_{j=1}^{I}\langle\delta[r_1-r_{ij}(t)]\delta[r_2-r_{ij}(0)]\rangle\tag{B9}$$

in expressions like Eq. B5 for the $S_{m,n}$, gives expressions for the $S_{m,n}$ in terms of $\langle C_i\rangle$, $P(i,r_p,r_q,t)$ and Dirac delta functions of differences of the r_p's, for $p, q = 1$ to $m+n$.

The function $P(i,r_1,r_2,t)$ is determined using the distribution function for the probability that a molecule of the ith species will be found at position r_1 at time t, given that it was at position r_2 at time zero (Aragón and Pecora, 1976). For molecules undergoing diffusion with coefficient D_i in the x,y-plane and/or translation along the y-axis,

$$\begin{aligned}P(i,r_1,r_2,t)&=\langle C_i\rangle\exp\left[-|r_1-r_2+jVt|^2/(4D_it)\right]/[4\pi D_it]\\P(i,r_1,r_2,0)&=\langle C_i\rangle\,\delta(r_1-r_2).\end{aligned}\tag{B10}$$

Furthermore, using Eq. 4 in Eq. B1, the $S_{m,n}$ can be written as sums of products of $f_{m',n'}$, where $m'+n'$ is less than $m+n$, and powers of $\langle C_i\rangle$. Using the two expressions for the $S_{m,n}$ yields

$$f_{1,1}(i,r_1,r_2;t)=P(i,r_1,r_2,t)$$

$$f_{1,2}(i,r_1,r_2,r_3;t)=\delta(r_2-r_3)P(i,r_1,r_2,t)$$

$$\begin{aligned}f_{2,2}(i,r_1,r_2,r_3,r_4;t)&=\delta(r_1-r_2)\delta(r_3-r_4)P(i,r_1,r_3,t)\\&+P(i,r_1,r_3,t)P(i,r_2,r_4,t)+P(i,r_1,r_4,t)P(i,r_2,r_3,t)\end{aligned}$$

$$f_{1,3}(i,r_1,r_2,r_3,r_4;t)=\delta(r_2-r_3)\delta(r_2-r_4)P(i,r_1,r_2,t)$$

$$\begin{aligned}&+\langle C_i\rangle\,[\delta(r_2-r_3)P(i,r_1,r_4,t)\\&+\delta(r_2-r_4)P(i,r_1,r_3,t)\\&+\delta(r_3-r_4)P(i,r_1,r_2,t)]\end{aligned}$$

$$\begin{aligned}&f_{2,3}(i,r_1,r_2,\ldots,r_5;t)\\&=\delta(r_1-r_2)\delta(r_3-r_4)\delta(r_3-r_5)P(i,r_1,r_3,t)\\&+\delta(r_3-r_4)[P(i,r_1,r_3,t)P(i,r_2,r_5,t)\\&\quad+P(i,r_1,r_5,t)P(i,r_2,r_3,t)]\\&+\delta(r_3-r_5)[P(i,r_1,r_3,t)P(i,r_2,r_4,t)\\&\quad+P(i,r_1,r_4,t)P(i,r_2,r_3,t)]\\&+\delta(r_4-r_5)[P(i,r_1,r_3,t)P(i,r_2,r_5,t)\\&\quad+P(i,r_1,r_5,t)P(i,r_2,r_3,t)]\\&+\langle C_i\rangle\,[\delta(r_1-r_2)\delta(r_3-r_4)P(i,r_1,r_5,t)\\&\quad+\delta(r_1-r_2)\delta(r_3-r_5)P(i,r_1,r_4,t)\\&\quad+\delta(r_1-r_2)\delta(r_4-r_5)P(i,r_1,r_3,t)]\end{aligned}$$

$$\begin{aligned}&f_{3,3}(i,r_1,r_2,\ldots,r_6;t)\\&=\delta(r_1-r_2)\delta(r_1-r_3)\delta(r_4-r_5)\delta(r_4-r_6)P(i,r_1,r_4,t)\\&+\delta(r_1-r_2)\delta(r_5-r_6)P(i,r_1,r_4,t)P(i,r_3,r_5,t)\\&\quad\text{and eight similar terms}\\&+\delta(r_1-r_2)\delta(r_4-r_5)P(i,r_1,r_4,t)P(i,r_3,r_6,t)\\&\quad\text{and eight similar terms}\\&+P(i,r_1,r_4,t)P(i,r_2,r_5,t)\,P(i,r_3,r_6,t)\\&\quad\text{and five similar terms}\\&+\langle C_i\rangle\delta(r_1-r_2)\delta(r_1-r_3)\delta(r_5-r_6)P(i,r_1,r_4,t)\\&\quad\text{and five similar terms}\\&+\langle C_i\rangle^2\delta(r_1-r_2)\delta(r_5-r_6)P(i,r_3,r_4,t)\\&\quad\text{and eight similar terms.}\end{aligned}\tag{B11}$$

The notation "similar" term refers to a different combination of positions that gives rise to an identical integrated term in Eq. 8. For example, in the second line of the above expression for $f_{3,3}$, another "similar" term is $\delta(r_1-r_3)\delta(r_5-r_6)P(i,r_1,r_4,t)P(i,r_2,r_5,t)$. The above expression for $f_{1,1}$ agrees with previously published results (Elson and Magde, 1974).

Using Eq. B10 to evaluate the values of $f_{m,n}$ at time zero, along with Eqs. 5 and 7, gives expressions for $\langle\delta C_i(r_1,0)\delta C_i(r_2,0)\ldots\delta C_i(r_n,0)\rangle$. Integrating these quantities over open observed area A_{obs} retrieves the moments about the mean of a Poisson distribution, as may be confirmed using the moment-generating function for the Poisson distribution (Abramowitz and Stegun, 1972),

$$\begin{aligned}\langle\delta N_i^n\rangle&=\left\langle\int_{A_{obs}}\delta C_i(r_{i1},0)\,d^2r_{i1}\cdot\int_{A_{obs}}\delta C_i(r_{i2},0)\,d^2r_{i2}\cdots\int_{A_{obs}}\delta C_i(r_{in},0)\,d^2r_{in}\right\rangle\\\langle\delta N_i\rangle&=0\\\langle\delta N_i^2\rangle&=\langle N_i\rangle\\\langle\delta N_i^3\rangle&=\langle N_i\rangle\\\langle\delta N_i^4\rangle&=\langle N_i\rangle+3\langle N_i\rangle^2\end{aligned}$$

$$\langle \delta N_i^5 \rangle = \langle N_i \rangle + 10\langle N_i \rangle^2$$
$$\langle \delta N_i^6 \rangle = \langle N_i \rangle + 25\langle N_i \rangle^2 + 15\langle N_i \rangle^3;$$
$$\langle N_i \rangle = \langle C_i \rangle A_{obs}. \quad \text{(B12)}$$

We thank Daniel Axelrod and Linda Spremulli for helpful discussions.

This work was supported by Grant GM-37145 from the National Institutes of Health, by the American Cancer Society Institutional Grant IN-15-28, by the University of North Carolina Research Council, by Presidential Young Investigator Award DCB8552986 from the National Science Foundation (N. Thompson), and by the University of North Carolina Board of Governors' Graduate Fellowship in Science and Technology (A. G. Palmer).

Received for publication 13 January 1987 and in final form 27 April 1987.

REFERENCES

Abramowitz, M., and I. A. Stegun, editors. 1972. Handbook of Mathematical Functions. National Bureau of Standards, Washington. 928–929.

Ackerson, B. J., T. W. Taylor, and N. A. Clark. 1985. Characterization of the local structure of fluids by apertured cross-correlation functions. *Phys. Rev. A.* 31:3183–3193.

Aragón, S. R., and R. Pecora. 1976. Fluorescence correlation spectroscopy as a probe of molecular dynamics. *J. Chem. Phys.* 64:1791–1803.

Axelrod, D., P. Ravdin, D. E. Koppel, J. Schlessinger, W. W. Webb, E. L. Elson, and T. R. Podleski. 1976*a*. Lateral motion of fluorescently labeled acetylcholine receptors in membranes of developing muscle fibers. *Proc. Natl. Acad. Sci. USA.* 73:4594–4598.

Axelrod, D., D. E. Koppel, J. Schlessinger, E. L. Elson, and W. W. Webb. 1976*b*. Mobility measurement by analysis of photobleaching recovery kinetics. *Biophys. J.* 16:1055–1069.

Borejdo, J. 1979. Motion of myosin fragments during actin-activated ATPase: fluorescence correlation spectroscopy study. *Biopolymers.* 18:2807–2820.

Borejdo, J., S. Putnam, and M. F. Morales. 1979. Fluctuations in polarized fluorescence: evidence that muscle cross bridges rotate repetitively during contraction. *Proc. Natl. Acad. Sci. USA.* 76:6346–6350.

Briggs, J., V. B. Elings, and D. F. Nicoli. 1981. Homogeneous fluorescent immunoassay. *Science (Wash. DC).* 212:1266–1268.

Cuatrecasas, P. 1983. Developing concepts in receptor research. *Drug Intell. Clin. Pharm.* 17:357–366.

Devore, J. L. 1982. Probability and Statistics for Engineering and the Sciences. Brooks/Cole Publishing Co., Monterey, CA. 258–300.

Due, C., M. Simonsen, and L. Olsson. 1986. The major histocompatibility complex class I heavy chain as a structural subunit of the human cell membrane insulin receptor: implications for the range of biological functions of histocompatibility antigens. *Proc. Natl. Acad. Sci. USA.* 83:6007–6011.

Elson, E. L., and D. Magde. 1974. Fluorescence correlation spectroscopy. I. Conceptual basis and theory. *Biopolymers.* 13:1–27.

Fahey, P. F., D. E. Koppel, L. S. Barak, D. E. Wolf, E. L. Elson, and W. W. Webb. 1977. Lateral diffusion in planar lipid bilayers. *Science (Wash. DC).* 195:305–306.

Fahey, P. F., and W. W. Webb. 1978. Lateral diffusion in phospholipid bilayer membranes and multilamellar liquid crystals. *Biochemistry.* 17:3046–3053.

Frieden, C. 1985. Actin and tubulin polymerization: the use of kinetic methods to determine mechanism. *Annu. Rev. Biophys. Biophys. Chem.* 14:189–210.

Gross, D., and W. W. Webb. 1986. Molecular counting of low-density lipoprotein particles as individuals and small clusters on cell surfaces. *Biophys. J.* 49:901–911.

Hirschfeld, T., and M. J. Block. 1977. Virometer: real time virus detection and identification in biological fluids. *Opt. Eng.* 16:406–407.

Hirschfeld, T., M. J. Block, and W. Mueller. 1977. Virometer: an optical instrument for visual observation, measurement and classification of free viruses. *J. Histochem. Cytochem.* 25:719–723.

Icenogle, R. D., and E. L. Elson. 1983*a*. Fluorescence correlation spectroscopy and photobleaching recovery of multiple binding reactions. I. Theory and FCS measurements. *Biopolymers.* 22:1919–1948.

Icenogle, R. D., and E. L. Elson. 1983*b*. Fluorescence correlation spectroscopy and photobleaching recovery of multiple binding reactions. II. FPR and FCS measurements at low and high DNA concentrations. *Biopolymers.* 22:1949–1966.

Koppel, D. E., D. Axelrod, J. Schlessinger, E. L. Elson, and W. W. Webb. 1976. Dynamics of fluorescence marker probe concentration as a probe of mobility. *Biophys. J.* 16:1315–1329.

Lanni, F., D. L. Taylor, and B. R. Ware. 1981. Fluorescence photobleaching recovery in solutions of labeled actin. *Biophys. J.* 35:351–364.

Leibovitch, L. S., and J. Fischbarg. 1985. Determining the kinetics of membrane pores from patch clamp data without measuring the open and closed times. *Biochim. Biophys. Acta.* 813:132–136.

Leibovitch, L. S., J. Fischbarg, and J. P. Koniarek. 1985. Optical correlation functions applied to the random telegraph signal: how to analyze patch clamp data without measuring the open and closed times. *Math. Biosci.* 76:1–13.

Leibovitch, L. S., and J. Fischbarg. 1986. Membrane pores: a computer simulation of interacting pores analyzed by $g_1(\tau)$ and $g_2(\tau)$ correlation functions. *J. Theor. Biol.* 119:287–297.

Magde, D., E. L. Elson, and W. W. Webb. 1972. Thermodynamic fluctuations in a reacting system—measurement by fluorescence correlation spectroscopy. II. *Phys. Rev. Lett.* 29:705–708.

Magde, D., W. W. Webb, and E. L. Elson. 1974. Fluorescence correlation spectroscopy. II. An experimental realization. *Biopolymers.* 13:29–61.

Metzger, H. 1978. The IgE-mast cell system as a paradigm for the study of antibody mechanisms. *Immunol. Rev.* 41:186–199.

Nicoli, D. F., J. Briggs, and V. B. Elings. 1980. Fluorescence immunoassay based on long time correlations of number fluctuations. *Proc. Natl. Acad. Sci. USA.* 77:4904–4908.

Oliver, C. J. 1981. Recent developments in photon correlation and spectrum analysis techniques. I. Instrumentation for photodetection spectroscopy. *In* Scattering Techniques Applied to Supramolecular and Nonequilibrium Systems. S. Chen, B. Chu, and R. Nossal, editors. Plenum Press, New York. 87–120.

Pastan, I. H., and M. C. Willingham. 1981. Receptor-mediated endocytosis of hormones in cultured cells. *Annu. Rev. Physiol.* 43:239–250.

Petersen, N. O. 1984. Diffusion and aggregation in biological membranes. *Can. J. Biochem. Cell Biol.* 62:1158–1166.

Petersen, N. O. 1986. Scanning fluorescence correlation spectroscopy. I. Theory and simulation of aggregation measurements. *Biophys. J.* 49:809–815.

Petersen, N. O., D. C. Johnson, and M. J. Schlesinger. 1986. Scanning fluorescence correlation spectroscopy. II. Application to virus glycoprotein aggregation. *Biophys. J.* 49:817–820.

Pomeau, Y. 1982. Symetrie des fluctuations dans le renversement du temps. *J. Physique.* 43:859–867.

Pusey, P. N. 1977. Statistical properties of scattered radiation. *In* Photon Correlation Spectroscopy and Velocimetry. H. Z. Cummins and E. R. Pike, editors. Plenum Press, New York. 45–141.

Roos, D. S., J. M. Robinson, and R. L. Davidson. 1983. Cell fusion and intramembranous particle distribution in polyethylene glycol resistant cells. *J. Cell Biol.* 97:909–917.

Saleh, B. 1978. Photoelectron Statistics. Springer-Verlag, Berlin. 25–40.

Salmon, E. D., W. M. Saxton, R. J. Leslie, M. L. Karow, and J. R. McIntosh. 1984. Diffusion coefficient of fluorescein-labeled tubulin in the cytoplasm of embryonic cells of a sea urchin: video image analysis of fluorescence redistribution after photobleaching. *J. Cell Biol.* 99:2157–2163.

Schlessinger, J., Y. Schechter, M. C. Willingham, and I. Pastan. 1978.

Direct visualization of binding, aggregation and internalization of insulin and epidermal growth factor on living fibroblastic cells. *Proc. Natl. Acad. Sci. USA.* 75:2659–2663.

Schreiber, A. B., J. Hoebke, B. Vray, and A. D. Strosberg. 1980. Evidence for reversible microclustering of lentil lectin membrane receptors on HeLa cells. *FEBS (Fed. Eur. Biochem. Soc.) Lett.* 111:303–306.

Shotton, D., K. Thompson, L. Wofsy, and D. Branton. 1978. Appearance and redistribution of surface proteins of the human erythrocyte membrane. *J. Cell Biol.* 76:512–531.

Sorscher, S. M., J. C. Bartholomew, and M. P. Klein. 1980. The use of fluorescence correlation spectroscopy to probe chromatin in the cell nucleus. *Biochim. Biophys. Acta.* 610:28–46.

Sorscher, S. M., and M. P. Klein. 1980. Profile of a focussed collimated laser beam near the focal minimum characterized by fluorescence correlation spectroscopy. *Rev. Sci. Instrum.* 51:98–102.

Steinberg, I. Z. 1986. On the time reversal of noise signals. *Biophys. J.* 50:171–179.

Suck, J. B., D. Quitmann, and B. Maier, editors. 1985. Workshop on investigation of higher order correlation functions. *J. Physique.* 46(C9):1–164.

Thompson, N. L., and D. Axelrod. 1983. Immunoglobulin surface binding kinetics studied by total internal reflection with fluorescence correlation spectroscopy. *Biophys. J.* 43:103–114.

Uster, P. S., and R. E. Pagano. 1986. Resonance energy transfer microscopy: observations of membrane-bound fluorescent probes in model membranes and in living cells. *J. Cell Biol.* 103:1221–1234.

Uzgiris, E. E., and R. D. Kornberg. 1983. Two-dimensional crystallization technique for imaging macromolecules, with application to antigen-antibody-complement complexes. *Nature (Lond.).* 301:125–129.

Wahl, P. 1985. Optimization of laser beams in FRAP experiments of microscopical objects. *Biophys. Chem.* 22:317–322.

Watts, T. H., H. E. Gaub, and H. M. McConnell. 1986. T-cell-mediated association of peptide antigen and major histocompatibility protein detected by energy transfer in an evanescent field. *Nature (Lond.).* 320:179–181.